

## Measurements of high-energy neutron-induced fission of $^{nat}\text{Pb}$ and $^{209}\text{Bi}$

D. Tarrío<sup>1,a</sup>, L. Tassan-Got<sup>2</sup>, L. Audouin<sup>2</sup>, B. Berthier<sup>2</sup>, I. Duran<sup>1</sup>, L. Ferrant<sup>2</sup>, S. Isaev<sup>2</sup>, C. Le Naour<sup>2</sup>, C. Paradela<sup>1</sup>, C. Stephan<sup>2</sup>, D. Trubert<sup>2</sup>, U. Abbondanno<sup>3</sup>, G. Aerts<sup>4</sup>, H. Álvarez<sup>1</sup>, F. Álvarez-Velarde<sup>5</sup>, S. Andriamonje<sup>6</sup>, J. Andrzejewski<sup>7</sup>, P. Assimakopoulos<sup>8</sup>, G. Badurek<sup>9</sup>, P. Baumann<sup>10</sup>, F. Becvár<sup>11</sup>, E. Berthoumieux<sup>6</sup>, F. Calviño<sup>12</sup>, M. Calviani<sup>13,14</sup>, D. Cano-Ott<sup>5</sup>, R. Capote<sup>15,16</sup>, C. Carrapiço<sup>17,6</sup>, P. Cennini<sup>18</sup>, V. Chepel<sup>19</sup>, E. Chiaveri<sup>18</sup>, N. Colonna<sup>20</sup>, G. Cortes<sup>12</sup>, A. Couture<sup>21</sup>, J. Cox<sup>21</sup>, M. Dahlfors<sup>18</sup>, S. David<sup>1</sup>, I. Dillmann<sup>22</sup>, C. Domingo-Pardo<sup>23,24</sup>, W. Dridi<sup>6</sup>, C. Eleftheriadis<sup>25</sup>, M. Embid-Segura<sup>5</sup>, A. Ferrari<sup>18</sup>, R. Ferreira-Marques<sup>19</sup>, K. Fujii<sup>3</sup>, W. Furman<sup>26</sup>, I. Gonçalves<sup>17</sup>, E. González-Romero<sup>5</sup>, F. Gramegna<sup>13</sup>, C. Guerrero<sup>5</sup>, F. Gunsig<sup>6</sup>, B. Haas<sup>27</sup>, R. Haight<sup>28</sup>, M. Heil<sup>22</sup>, A. Herrera-Martinez<sup>18</sup>, M. Igashira<sup>29</sup>, E. Jericha<sup>9</sup>, Y. Kadi<sup>18</sup>, F. Käppeler<sup>22</sup>, D. Karadimos<sup>8</sup>, D. Karamanis<sup>8</sup>, M. Kerveno<sup>10</sup>, P. Koehler<sup>30</sup>, E. Kossionides<sup>31</sup>, M. Krťicka<sup>11</sup>, C. Lampoudis<sup>25,6</sup>, H. Leeb<sup>9</sup>, A. Lindote<sup>19</sup>, I. Lopes<sup>19</sup>, M. Lozano<sup>16</sup>, S. Lukic<sup>10</sup>, J. Marganec<sup>7</sup>, S. Marrone<sup>20</sup>, T. Martínez<sup>5</sup>, C. Massimi<sup>32</sup>, P. Mastinu<sup>13</sup>, A. Mengoni<sup>15,18</sup>, P.M. Milazzo<sup>3</sup>, C. Moreau<sup>3</sup>, M. Mosconi<sup>22</sup>, F. Neves<sup>19</sup>, H. Oberhammer<sup>9</sup>, S. O'Brien<sup>21</sup>, M. Oshima<sup>33</sup>, J. Pancin<sup>6</sup>, C. Papachristodoulou<sup>8</sup>, C. Papadopoulos<sup>34</sup>, N. Patronis<sup>8</sup>, A. Pavlik<sup>35</sup>, P. Pavlopoulos<sup>36</sup>, L. Perrot<sup>6</sup>, M.T. Pigni<sup>9</sup>, R. Plag<sup>22</sup>, A. Plompen<sup>37</sup>, A. Plukis<sup>6</sup>, A. Poch<sup>12</sup>, J. Praena<sup>13</sup>, C. Pretel<sup>12</sup>, J. Quesada<sup>16</sup>, T. Rauscher<sup>38</sup>, R. Reifarth<sup>28</sup>, C. Rubbia<sup>39</sup>, G. Rudolf<sup>10</sup>, P. Rullhusen<sup>37</sup>, J. Salgado<sup>17</sup>, C. Santos<sup>17</sup>, L. Sarchiapone<sup>18</sup>, I. Savvidis<sup>25</sup>, G. Tagliente<sup>20</sup>, J.L. Tain<sup>23</sup>, L. Tavora<sup>17</sup>, R. Terlizzi<sup>20</sup>, G. Vannini<sup>32</sup>, P. Vaz<sup>17</sup>, A. Ventura<sup>40</sup>, D. Villamarin<sup>5</sup>, M.C. Vicente<sup>5</sup>, V. Vlachoudis<sup>18</sup>, R. Vlastou<sup>34</sup>, F. Voss<sup>22</sup>, S. Walter<sup>22</sup>, M. Wiescher<sup>21</sup>, and K. Wisshak<sup>22</sup> (The n\_TOF Collaboration ([www.cern.ch/ntof](http://www.cern.ch/ntof)))

<sup>1</sup> Universidad de Santiago de Compostela, Spain

<sup>2</sup> Centre National de la Recherche Scientifique/IN2P3-IPN, Orsay, France

<sup>3</sup> Istituto Nazionale di Fisica Nucleare, Trieste, Italy

<sup>4</sup> CEA/Saclay – IRFU, Gif-sur-Yvette, France

<sup>5</sup> Centro de Investigaciones Energeticas Medioambientales y Tecnologicas, Madrid, Spain

<sup>6</sup> CEA/Saclay – DSM/DAPNIA, Gif-sur-Yvette, France

<sup>7</sup> University of Lodz, Lodz, Poland

<sup>8</sup> University of Ioannina, Greece

<sup>9</sup> Atominstytut der Österreichischen Universitäten, Technische Universität

<sup>10</sup> Centre National de Recherche Scientifique/IN2P3 – IrS, Strasbourg, France

<sup>11</sup> Charles University, Prague, Czech Republic

<sup>12</sup> Universidad Politecnica de Catalunya, Barcelona, Spain

<sup>13</sup> Istituto Nazionale di Fisica Nucleare, Laboratori Nazionali di Legnaro, Italy

<sup>14</sup> Dipartimento di Fisica, Università di Padova, Italy

<sup>15</sup> International Atomic Energy Agency (IAEA), Nuclear Data Section, Vienna, Austria

<sup>16</sup> Universidad de Sevilla, Spain

<sup>17</sup> Instituto Tecnológico e Nuclear (ITN), Lisbon, Portugal

<sup>18</sup> CERN, Geneva, Switzerland

<sup>19</sup> LIP – Coimbra, Departamento de Fisica da Universidade de Coimbra, Portugal

<sup>20</sup> Istituto Nazionale di Fisica Nucleare, Bari, Italy

<sup>21</sup> University of Notre Dame, Notre Dame, USA

<sup>a</sup> e-mail: [diego.tarrío@usc.es](mailto:diego.tarrío@usc.es)

- <sup>22</sup> Karlsruhe Institute of Technology (KIT), Campus Nord, GmbH (FZK), Institut für Kernphysik, Germany
- <sup>23</sup> Instituto de Física Corpuscular, CSIC-Universidad de Valencia, Spain
- <sup>24</sup> GSI, Darmstadt, Germany
- <sup>25</sup> Aristotle University of Thessaloniki, Greece
- <sup>26</sup> Joint Institute for Nuclear Research, Frank Laboratory of Neutron Physics, Dubna, Russia
- <sup>27</sup> Centre National de la Recherche Scientifique/IN2P3-CENBG, Bordeaux, France
- <sup>28</sup> Los Alamos National Laboratory, New Mexico, USA
- <sup>29</sup> Tokyo Institute of Technology, Tokyo, Japan
- <sup>30</sup> Oak Ridge National Laboratory, Physics Division, Oak Ridge, USA
- <sup>31</sup> NCSR, Athens, Greece
- <sup>32</sup> Dipartimento di Fisica, Università de Bologna, and Sezione INFN di Bologna, Italy
- <sup>33</sup> Japan Atomic Energy Research Institute, Tokai-mura, Japan
- <sup>34</sup> National Technical University of Athens, Greece
- <sup>35</sup> Fakultät für Physik, Universität Wien, Austria
- <sup>36</sup> Pôle Universitaire Léonard de Vinci, Paris, La Défense, France
- <sup>37</sup> CEC-JRC-IRMM, Geel, Belgium
- <sup>38</sup> Department of Physics – University of Basel, Switzerland

**Abstract.** The CERN Neutron Time-Of-Flight (n\_TOF) facility is well suited to measure low cross sections as those of neutron-induced fission in subactinides. The cross section ratios of  $^{nat}\text{Pb}$  and  $^{209}\text{Bi}$  relative to  $^{235}\text{U}$  and  $^{238}\text{U}$  were measured using PPAC detectors and a fragment coincidence method that allows us to identify the fission events. The present experiment provides first results for neutron-induced fission up to 1 GeV. Good agreement is found with previous experimental data below 200 MeV. The comparison with proton-induced fission indicates that the limiting regime where neutron-induced and proton-induced fission reach equal cross sections is close to 1 GeV.

## 1 Introduction

The development of Accelerator Driven Systems (ADS) requires a good knowledge of the cross sections for a variety of reactions. In particular, neutron-induced fission cross sections of  $^{nat}\text{Pb}$  and  $^{209}\text{Bi}$  are of special interest since they will probably be the main compound materials of the spallation target [1]. In consequence, the neutron spectrum and the radioactivity produced in the target will be significantly affected by neutron-induced fission of Pb and Bi.

Another application for  $^{209}\text{Bi}$  is in neutron fluence monitors. Thanks to its high fission threshold of about 20 MeV it can be used even in a background of low energy neutrons. The fact that bismuth is a monoisotopic and non-radioactive material suggests that the  $^{209}\text{Bi}(n,f)$  reaction might be considered a well-suited standard cross section [2]. However, due to the technical difficulties to obtain neutron beams of high energy, the available evaluations of (n,f) cross section have been made using experimental data below 200 MeV. The present work at the CERN n\_TOF facility provides first results of the neutron-induced fission cross sections of  $^{nat}\text{Pb}$  and  $^{209}\text{Bi}$  in an extended energy range up to 1 GeV.

## 2 The experimental setup

The present experiment has been performed at the n\_TOF (neutron Time-Of-Flight) facility at CERN, where a very intense neutron beam is produced by spallation reactions on a lead target, using a 20 GeV/c proton beam from the PS (Proton Synchrotron) at CERN. The water of the cooling system acts as a moderator to produce the extended energy range of the neutron flux from thermal up to several GeV. Up to now, n\_TOF is the only facility that reaches such high neutron energies. The 185 m flight path between the spallation target and the experimental area allows one to measure the neutron

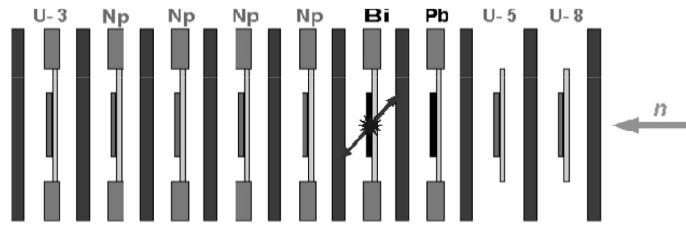


Fig. 1. Schematic view of the PPAC detection setup used in this experiment.

energy with a high accuracy (6% around 1 GeV and 0.01% around 1 eV). A more detailed description of the n\_TOF facility can be found in Ref. [3].

The experimental setup used in this experiment consisted in a reaction chamber especially designed for this purpose housing 10 PPAC (Parallel Plate Avalanche Counter) detectors. Each PPAC has a central anode surrounded by two cathodes with a low-pressure gas filling the gaps between the electrodes. The cathodes are segmented in orthogonal directions so that the fission fragments trajectory can be reconstructed. Thin targets were placed in between the PPACs as shown in Fig. 1, where targets of  $^{235}\text{U}$  and  $^{238}\text{U}$  were included as references.

A detailed characterisation of the targets used in this experiment, including the values of the total masses, and their chemical composition has been performed by means of Rutherford Backscattering Spectroscopy (RBS). Additional measurements of the  $\alpha$ -activity of the radioactive samples provided an independent measurement of the target masses and of their spatial distribution.

### 3 Data analysis

Fission events were identified by coincident detection of the fragments within a time window of 10 ns. This constraint discards most of the background due to the  $\alpha$ -activity of the radioactive targets and to the emission of light particles in spallation reactions.

For a single target, the number of detected fission events is given by:

$$C_i(E) = \Phi_i(E) \cdot N_i \cdot \sigma_i(E) \cdot \varepsilon_i(E) \quad (1)$$

where  $\Phi(E)$  is the neutron fluence (in  $n/\text{cm}^2$ ) integrated for the full measuring time,  $N$  is the total number of atoms in the target,  $\sigma(E)$  is the fission cross section and  $\varepsilon(E)$  is the detection efficiency. Therefore, the cross section ratio of two of the targets can be calculated from Equation 1, as:

$$\frac{\sigma_i(E)}{\sigma_j(E)} = \frac{C_i(E)}{C_j(E)} \cdot \frac{\Phi_j(E)}{\Phi_i(E)} \cdot \frac{N_j}{N_i} \cdot \frac{\varepsilon_j(E)}{\varepsilon_i(E)} \quad (2)$$

The PPACs and the targets are so thin that the neutron flux attenuation is less than 1%, as demonstrated by MCNP calculations [4] so that the ratio  $\Phi_j(E)/\Phi_i(E)$  can be assumed as 1 for samples of the same size. However, the reference samples of  $^{235}\text{U}$  and  $^{238}\text{U}$  were 8 cm in diameter, while  $^{\text{nat}}\text{Pb}$  and  $^{209}\text{Bi}$  were spread over the whole backing surface. Using the cathode signals it is possible to map the fission events over the target area and, in this way, to obtain the correction on the neutron fluence for different samples, when needed, as it can be seen in Fig. 2 for  $^{209}\text{Bi}$  and  $^{235}\text{U}$  targets. The figure also shows that the beam spot is shifted upward with respect to the nominal position of the neutron beam, represented by the black circles.

The detection efficiencies  $\varepsilon(E)$  for the various targets differ slightly due to differences in the backings and in the sample thicknesses. A simulation combining Monte-Carlo methods and numerical calculations for the stopping power was developed to estimate these corresponding ratios  $\varepsilon_j(E)/\varepsilon_i(E)$ , where the different mass distribution of the fission fragments was also taken into account. The efficiency ratios  $\varepsilon_{\text{U}235}(E)/\varepsilon_{\text{Pb}}(E)$  and  $\varepsilon_{\text{U}235}(E)/\varepsilon_{\text{Bi}209}(E)$  were estimated to 0.85, while the  $\varepsilon_{\text{U}238}(E)/\varepsilon_{\text{Pb}}(E)$  and  $\varepsilon_{\text{U}238}(E)/\varepsilon_{\text{Bi}209}(E)$  ratios were estimated to 0.88. Due to the limited angular acceptance of the experimental setup, our data have been corrected using the parameterization proposed in Ref. [5] for the

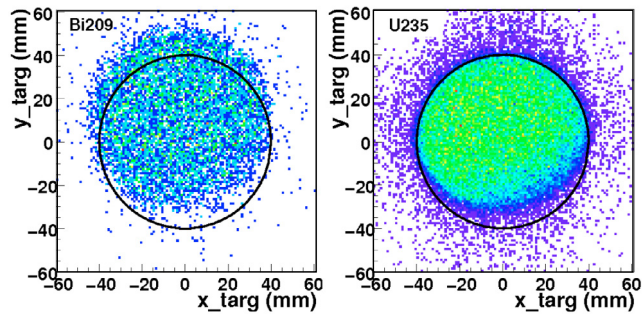


**Fig. 2.** Position of the fission events in the  $^{209}\text{Bi}$  and in the  $^{235}\text{U}$  samples. The black circles represent the nominal position of the neutron beam.

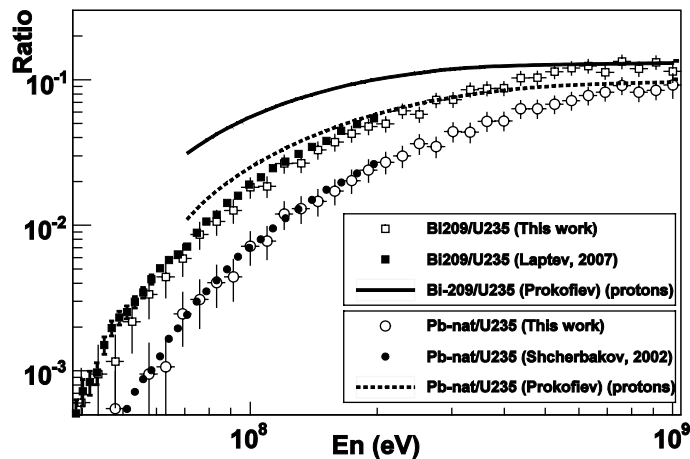


**Fig. 3.** Ratios of the neutron-induced fission cross sections of  $^{\text{nat}}\text{Pb}/^{235}\text{U}$  and  $^{209}\text{Bi}/^{235}\text{U}$  obtained in this work (solid symbols), compared with some previous data from [6, 7] (open symbols). The solid and dashed lines are the corresponding ratios for proton-induced fission from the systematic of Ref. [8].

anisotropy. The overall contribution of systematic uncertainties has been estimated to be lower than 12%, including the effect of the linear momentum transferred from the incident neutrons to the nuclei, what has been calculated to be much lower than the other components of the systematic uncertainty.

## 4 Results

We have measured the neutron-induced fission cross sections of  $^{\text{nat}}\text{Pb}$  and  $^{209}\text{Bi}$  relative to  $^{235}\text{U}$  and to  $^{238}\text{U}$  from threshold up to 1 GeV. The ratios of the (n,f) cross sections of  $^{\text{nat}}\text{Pb}$  and  $^{209}\text{Bi}$  with respect to  $^{235}\text{U}$  are shown in Fig. 3. The error bars represent the statistical uncertainties only, being the systematic related uncertainties below 12%. Good agreement is found with previous results from Refs. [6, 7] which cover the energy range below 200 MeV. Above this energy, only data for proton-induced fission are available. Therefore, the ratios obtained from the systematics presented in [8] for proton-induced fission are shown for comparison.

To obtain the final cross sections of  $^{\text{nat}}\text{Pb}(n,f)$  and  $^{209}\text{Bi}(n,f)$ , the ratios were multiplied by the  $^{235}\text{U}(n,f)$  and  $^{238}\text{U}(n,f)$  cross sections given by the JENDL/HE-2007 evaluation, the only one that covers the whole energy range of our data. The results obtained with the two reference cross sections are compatible. The final values of the cross sections are shown in Figs. 4 and 5.

For both isotopes,  $^{\text{nat}}\text{Pb}$  and  $^{209}\text{Bi}$ , our results are compatible with previous measurements below 200 MeV in Refs. [7, 9, 10]. The presently available evaluations agree well with our data below

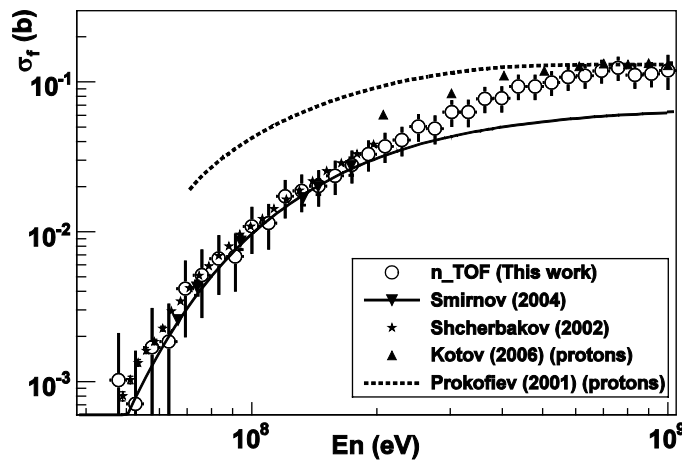


Fig. 4. Neutron-induced fission cross section of  $^{nat}\text{Pb}$  obtained in this work, compared with previous data from [7,9]. Experimental data [11] and systematics [8] for proton-induced fission are also shown.

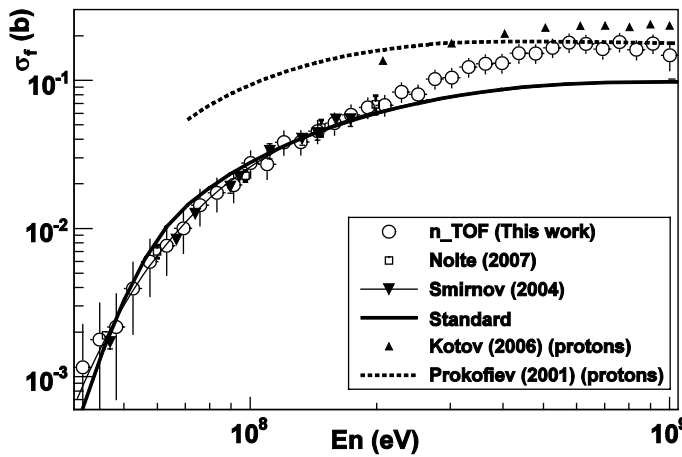


Fig. 5. Neutron-induced fission cross section of  $^{209}\text{Bi}$  obtained in this work, compared with previous data from [9,10]. The parametrization from Smirnov et al. [9] and the recommended standard cross section of Carlson et al. [2] do not reproduce our data above 200 MeV. Experimental data [11] and systematics [8] for proton-induced fission are also shown.

200 MeV, but deviate significantly at higher energies. In both cases the parameterization proposed by Smirnov et al. [9] is shown, while for the  $^{209}\text{Bi}(n,f)$  case also the recommended standard cross section of Carlson et al. [2] has been included. On the basis of the new results, a revision of the evaluations is clearly called for.

Experimental data for proton-induced fission from [11], as well as the systematics of Prokofiev [8] are shown for comparison. It can be inferred that the  $(n,f)$  cross sections, even though they are lower than the  $(p,f)$  values at lower energy, tend to be compatible with around 1 GeV.

## 5 Summary and conclusions

Taking advantage of the intense, white neutron source n\_TOF at CERN, and of the timing capabilities of the PPAC detectors, the neutron-induced fission cross sections of  $^{nat}\text{Pb}$  and  $^{209}\text{Bi}$  have been measured, for the first time, from threshold up to 1 GeV. The results are in good agreement with previous data and existing evaluations below 200 MeV but deviate significantly at higher energies. Therefore,

the evaluations should be revised above 200 MeV to comply with the present experimental values. The results tend to be compatible with the (p,f) values around 1 GeV.

## References

1. OECD-NEA, “*Accelerator and Spallation Target Technologies for ADS Applications: Status Report*”, NEA-5421 (2005)
2. A.D. Carlson, S. Chiba, F.J. Hambsch, N. Olsson and A.N. Smirnov, “*Update to Nuclear Data Standards for Nuclear Measurements*”, IAEA Report INDC (NDS), p. 368 (1997)
3. The n\_TOF Collaboration, “*CERN n\_TOF Facility: Performance Report*”, CERN/INTC-O-011, CERN-SL-2002-053 ECT (2002)
4. L. Ferrant, PhD. Work, Université Paris-Sud (2005)
5. V.P. Eismont, A.V. Prokofiev, I.V. Ryzhov et al., “*Proc. of the 3<sup>rd</sup> International Conference on Accelerator Driven Transmutation technologies and Applications*”, Praha, Czech Republic (1999)
6. A.B. Laptev et al., “*Proc. Of the 4<sup>th</sup> International Conference on Fission and Properties of Neutron-Rich Nuclei*”, Sanibel Island, Florida (2007)
7. O. Shcherbakov et al., *Journ. Nucl. Sci. and Techn.*, **Supp. 2**, 230 (2002)
8. A.V. Prokofiev, *Nucl. Inst. and Meth. A*, **463**, 557 (2001)
9. A.N. Smirnov et al., *Phys. Rev. C*, **70**, 054603 (2004)
10. R. Nolte et al., *Nucl. Sci. Eng.*, **156**, 197 (2007)
11. A.A. Kotov et al, *Phys. Rev. C*, **74**, 034605 (2006)